IOPscience iopscience.iop.org

Home Search Collections Journals About Contact us My IOPscience

Molecular motor efficiency is maximized in the presence of both power-stroke and rectification through feedback

This content has been downloaded from IOPscience. Please scroll down to see the full text.

2015 New J. Phys. 17 065011

(http://iopscience.iop.org/1367-2630/17/6/065011)

View the table of contents for this issue, or go to the journal homepage for more

Download details:

IP Address: 147.96.14.15
This content was downloaded on 22/09/2015 at 19:24

Please note that terms and conditions apply.

IOP Publishing New J. Phys. 17 (2015) 065011 doi:10.1088/1367-2630/17/6/065011

New Journal of Physics
The open access journal at the forefront of physics

Deutsche Physikalische Gesellschaft DPG
IOP Institute of Physics

Published in partnership with: Deutsche Physikalische Gesellschaft and the Institute of Physics

OPEN ACCESS

RECEIVED
19 March 2015

REVISED
30 April 2015

ACCEPTED FOR PUBLICATION
18 May 2015

PUBLISHED
15 June 2015

Content from this work may be used under the terms of the Creative Commons Attribution 3.0 licence.

Any further distribution of this work must maintain attribution to the author(s) and the title of the work, journal citation and DOI.

PAPER

Molecular motor efficiency is maximized in the presence of both power-stroke and rectification through feedback

R K Schmitt[1], **J M R Parrondo**[2], **H Linke**[1] **and J Johansson**[1]

[1] Solid State Physics and Nanometer Structure Consortium (nm C@ LU), Lund University, PO Box 118, SE-221 00 Lund, Sweden
[2] Departamento de Fisica Atómica, Molecular y Nuclear and GISC, Universidad Complutense de Madrid, E-28040 Madrid, Spain

E-mail: regina.schmitt@ftf.lth.se

Keywords: molecular motor, Brownian ratchet, power-stroke, rectification of fluctuations, efficiency, Shannon entropy, Brownian recitifier

Abstract

We present a model for a feedback-controlled ratchet consisting of a Brownian particle and a moving, finite barrier that is shifted by an external agent depending on the position of the particle. By modifying the value of a single parameter of the feedback protocol, the model can act either as a pure rectifier, a power-stroke (PS) motor, or a combination of both. Interestingly, in certain situations the motor reaches a maximum efficiency for an intermediate value of that parameter, i.e., for a combination of the information ratchet and the PS mechanisms. We relate our results to the biological motors kinesin, myosin II, and myosin V, finding that these motors operate in a regime of length scales and forces where the efficiency is maximized for a combination of rectification and PS mechanisms.

1. Introduction

Molecular motors perform many tasks in all living species, such as muscle movement, cell division, and the transport of molecules and ions across the cell membrane. They are protein complexes that transduce chemical energy into mechanical work, usually by hydrolysis of ATP to ADP and inorganic phosphate. Due to the high efficiency of these transduction processes, molecular motors are of tremendous interest and inspiration for research on artificial bio-machines. Focusing here on translational motors from a biophysics perspective, two main mechanisms are commonly discussed: first, the power-stroke (PS) mechanism, where the ATP consumption is thought of as leading to a conformational change, actively pushing the motor forward [1]. Second, a rectification process, in which the ATP hydrolysis is used to rectify thermal fluctuations. The latter was suggested as early as 1957 by Huxley [2] and is sometimes referred to as a 'Brownian ratchet'. Because the expression 'Brownian ratchet' is ambiguous in the literature we will rather use the term 'Brownian rectifier' (BR) to clearly distinguish the two mechanisms that are described above. The two types of motors show different responses to external load [3] and can even induce opposite collective behaviors when several motors work together [4].

In this paper we analyze the performance of the two mechanisms in a simple one-particle model that exhibits a crossover between the PS and the BR behavior. We use a feedback control protocol that activates a rectification mechanism depending on the position of the particle. Such feedback protocols have been extensively studied in the context of the Maxwell's demon and the thermodynamics of information [5, 6]. In real biological motors, on the other hand, there is no external agent, that measures and implements the feedback protocol. Instead, feedback is implemented by a reaction or configuration change that takes place only when the motor reaches certain positions. For instance, for effective processive motion of bipedal motors, the coupling between the state of the motor and the next reaction step is crucial; this coupling needs a feedback mechanism (without an external agent). In the case of myosin V, feedback is thought to be implemented by mechanical strain internal to the molecule, such that binding of the leading head increases the unbinding rate of the trailing head[7, 8]. Likewise, several studies support the idea that intramolecular tension might serve as a feedback mechanism for kinesin [9]. Feedback could then be implemented as structural or chemical changes that lead to asymmetric

© 2015 IOP Publishing Ltd and Deutsche Physikalische Gesellschaft

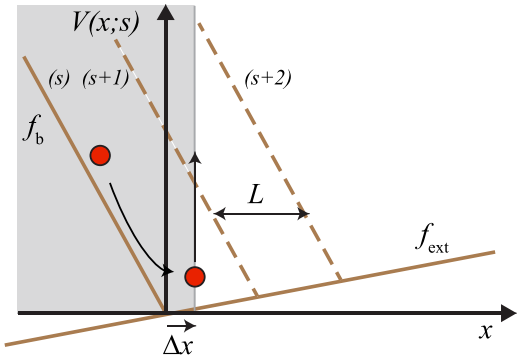

Figure 1. Model system: particle moving in a potential characterized through the external force f_{ext} and the barrier slope f_b, the control value Δx and the distance between barriers L. Displayed is the case $0 < \Delta x < L$ (intermixing regime). The dotted lines indicate the system in state $s + 1$ and $s + 2$.

unbinding and binding rates between front and rear head. These asymmetric rates are another way of describing the movement of molecular motors, as in [10]. The analysis of biological processes as feedback protocols introduces a new perspective and, in particular, allows one to assess the minimal energetic cost of the feedback process [6] independently of the specific chemical or physical mechanism that induces the feedback.

Our model consists of a particle diffusing freely in a piecewise linear potential coupled to a feedback control system. Depending on the position of the particle in relation to a specific control value Δx, potential barriers are set up at predetermined positions. A similar model with infinite barriers has been analyzed as a pure information motor that can rectify fluctuations converting information into work [11, 12]. In our case, the barrier slope is finite and the barrier can thus push the particle for certain values of Δx. Thereby the control value determines whether the BR or the PS mechanism dominates and this allows us to analyze the performance of the two mechanisms. Interestingly, the control value that maximizes the efficiency of the motor corresponds to, in certain situations, a combination of the two mechanisms.

The paper is organized as follows. We introduce the model and discuss the energetics and the efficiency of the motor in section 2. In section 3, we present an analytical solution that is exact when the system is allowed to relax to equilibrium between measurements. By comparing with numerical simulations, we conclude that the equilibrium limit is the optimal regime regarding efficiency. In section 4, we analyze the length scale regime of real biological motors with regard to the previous results. Finally, in section 5 we summarize our main results and present our conclusions.

2. Model

Consider a Brownian particle moving in one dimension against an external force $-f_{ext} \leqslant 0$ pointing to the left (see figure 1). Our motor is a simple ratchet model in which a barrier is shifted a fixed length L to the right, when the particle reaches a certain position due to thermal fluctuations [11].

The barrier exerts a finite force $f_{motor} \geqslant 0$ when the particle is below the barrier location Ls, with $s = 0, 1, 2, \ldots$ The potential associated with the barrier reads

$$V_b(x; s) = -f_{motor}(x - Ls)\Theta(Ls - x), \tag{1}$$

where $\Theta(x)$ is the step function: $\Theta(x) = 1$ for $x \geqslant 0$ and 0 otherwise. The total potential acting on the particle is (see figure 1):

$$V(x; s) = V_b(x; s) + f_{ext}x = \begin{cases} -f_b(x - Ls) + f_{ext}\,Ls & \text{for } x < Ls, \\ f_{ext}\,x & \text{for } x \geqslant Ls, \end{cases} \tag{2}$$

where we have introduced the slope of the potential in the barrier $f_b = f_{motor} - f_{ext} \geqslant 0$, which is the parameter that measures the strength of the barrier in our model.

The system is coupled to a thermal bath at temperature T. The state variable s is controlled by an external agent according to the following feedback protocol, sketched in figure 1: the agent measures the position $x_n \equiv x(nt_m)$ of the particle at regular intervals of time nt_m, with n integer; if the particle is observed above a certain control distance $Ls + \Delta x$, the barrier potential is shifted to the right a distance L, i.e., $V_b(x; s) \to V_b(x; s + 1)$ if $x_n \equiv x(nt_m) \geqslant Ls + \Delta x$. Otherwise, the potential remains unaltered. The operation

mechanism of the motor depends on the value of the threshold Δx. For $\Delta x \ll 0$, the switching condition $x_n \geqslant Ls + \Delta x$ is fulfilled with high probability. Therefore, the measurement is irrelevant (the information provided by the measurement is negligible) and the feedback algorithm always shifts the barrier upon measurement. This regime corresponds to a PS motor that performs work on the particle by pushing it, using the barrier slope against the external force. On the other hand, for $\Delta x \geqslant L$, the barrier is shifted with zero work, because the particle is above the new barrier position, $x_n \geqslant L(s+1)$. In this limit, the motor acts as a pure BR, which uses information about the particle position to rectify thermal fluctuations. The performance of these two disparate regimes can be compared using a generalized efficiency that incorporates the energetic cost of the two mechanisms: pushing and feedback.

Thermodynamics of information [6] states that the minimum work to perform a series of error-free measurements is given by H, where H is the Shannon entropy of the outcomes. Although it is not easy to find a specific physical mechanism that achieves this minimum work in a feedback process [12], Shannon entropy provides a general tool to quantify the efficiency of feedback [6, 13]. In our case, we can consider the measurement outcomes as binary random variables: $o_n = 1$ if $x_n \geqslant Ls + \Delta x$ (switch), and $o_n = 0$ otherwise (no switch). The minimum average work per measurement is given by $W_{\text{info}} = kTh$, where h is the Shannon information per measurement, or information rate of the binary string $\{o_n\}$ [14]. More precisely, if the joint probability to observe a given sequence of outcomes in l measurements is $P[\{o_i\}_n^{n+l}] \equiv p(o_n, o_{n+1}, \ldots, o_{n+l})$, then the Shannon entropy is given by

$$H_l = -\sum_{\{o_i\}=0,1} P\left[\{o_i\}_n^{n+l}\right] \ln P\left[\{o_i\}_n^{n+l}\right] \tag{3}$$

and the information rate is given by

$$h = \lim_{l\to\infty} \frac{H_l}{l}. \tag{4}$$

An alternative expression reads:

$$h = \lim_{l\to\infty} \left[H_{l+1} - H_l\right], \tag{5}$$

which exhibits a faster convergence and is therefore more suitable for numerical estimations [15]. Notice that the information rate accounts for possible correlations among subsequent outcomes, which can be relevant for small t_m.

The energetics is completed by the average input work due to the potential shift:

$$W_{\text{in}} = \left\langle o_n \left[V(x_n; s+1) - V(x_n; s)\right]\right\rangle, \tag{6}$$

as well as by the output work or average gain of potential energy:

$$W_{\text{out}} = \left\langle f_{\text{ext}}(x_{n+1} - x_n)\right\rangle = \left\langle o_n \right\rangle f_{\text{ext}} L, \tag{7}$$

where the averages are taken over the position x_n (note that $o_n = \Theta(x_n - Ls - \Delta x)$ is a function of x_n). In (7), we have further assumed that the system has reached a steady state where $\langle x_{n+1} - x_n\rangle = L$ if the measurement induces a switch ($o_n = 1$) and $\langle x_{n+1} - x_n\rangle = 0$ otherwise ($o_n = 0$).

Finally, the efficiency of the motor is given by:

$$\eta = \frac{W_{\text{out}}}{W_{\text{in}} + W_{\text{info}}} = \frac{W_{\text{out}}}{W_{\text{in}} + kTh}. \tag{8}$$

As mentioned above, for $\Delta x \ll 0$, $h \simeq 0$ and we recover the standard definition of efficiency for a non-feedback Brownian motor. On the other hand, for $\Delta x \geqslant L$, W_{in} is identically zero, and the efficiency coincides with the one introduced in [5, 13] for pure information motors. Notice that Δx and L are key parameters for our discussion on the efficiency of the PS and the BR mechanisms and we want to be able to change them independently. Therefore, we set an arbitrary unit of length u for Δx, x and L; energies are given in terms of kT and forces are expressed in units kT/u.

2.1. Analytical solution for low-frequency measurements

In the limit of infinite waiting times between measurements, $t_m \to \infty$, the particle will reach equilibrium between two measurements and the model can be solved analytically. In that case the probability density of the particle position, immediately before the measurement, is given by a canonical distribution:

$$\rho(x; s) = \frac{1}{Z(s)} e^{-\beta V(x;s)}, \tag{9}$$

with $\beta = 1/kT$ and the partition function

$$Z(s) = \int_{-\infty}^{\infty} \mathrm{e}^{-\beta V(x;s)}\,\mathrm{d}x = \frac{f_\mathrm{b} + f_\mathrm{ext}}{\beta f_\mathrm{b} f_\mathrm{ext}}\,\mathrm{e}^{-\beta L s f_\mathrm{ext}}. \tag{10}$$

The applied work W_in, the gained potential energy W_out, and the energy associated with the entropy rate W_info can be calculated as expectation values, where only the part of the distribution $\rho(x;\,s)\Theta(x-\Delta x)$ contributes, because no work is done on the particle if it has not passed the control value. Then

$$W_\mathrm{in} = \int_{Ls+\Delta x}^{\infty} \rho(x;\,s)\,[V(x;\,s+1) - V(x;\,s)]\,\mathrm{d}x, \tag{11}$$

$$W_\mathrm{out} = p\,f_\mathrm{ext} L, \tag{12}$$

where p is the probability that the particle has passed the control value Δx:

$$\begin{aligned} p \equiv \langle o_n \rangle &= \int_{Ls+\Delta x}^{\infty} \rho(x;\,s)\,\mathrm{d}x \\ &= \begin{cases} \frac{f_\mathrm{b}}{f_\mathrm{b}+f_\mathrm{ext}}\,\exp\left[-\beta f_\mathrm{ext}\Delta x\right] & \text{for } \Delta x \geqslant 0, \\ 1 - \frac{f_\mathrm{ext}}{f_\mathrm{b}+f_\mathrm{ext}}\,\exp\left[\beta f_\mathrm{b}\Delta x\right] & \text{for } \Delta x \leqslant 0. \end{cases} \end{aligned} \tag{13}$$

In the limit of large times t_m between measurements, every measuring event is independent and the entropy rate h is given by the Shannon entropy of a single outcome, yielding

$$W_\mathrm{info} = kT\,[-p\,\ln p - (1-p)\ln(1-p)]. \tag{14}$$

2.2. Numerical simulations

For finite t_m, we study the motor dynamics solving the corresponding overdamped Langevin equation

$$\frac{\mathrm{d}x}{\mathrm{d}t} = -\beta D\frac{\partial V}{\partial x} + \zeta(t), \tag{15}$$

where D is the diffusivity and $\zeta(t)$ is a Gaussian white noise with zero average and correlation given by

$$\langle \zeta(t')\zeta(t)\rangle = 2D\delta(t-t'). \tag{16}$$

In time intervals t_m, the position of the particle is measured and the feedback protocol is implemented as described above. The average input and output work are calculated using (6) and (7), respectively.

The estimation of the information rate, h, of the string of outcomes, given by (5), is difficult from a computational point of view because the string can exhibit longterm correlations. To resolve this difficulty, we map the original binary string $S \equiv \{o_n\}$ onto a new string S_0 (S_1) of natural numbers counting the number of zeros (ones) between consecutive ones (zeros). For example, the two maps acting on the outcome string

$$S = 100100011011100$$

result, respectively, in the strings

$$S_0 = 230100, \qquad S_1 = 0100230.$$

Because these maps are one-to-one, S, S_0 and S_1 all carry exactly the same information: $H(S) = H(S_0) = H(S_1)$. Given a binary string S with length l, the length l_1 (l_0) of the resulting string S_1 (S_0) is equal to the number of zeros (ones) in S. Thus, if $p = \langle o_n \rangle$ is the probability to switch the potential, the average length of the new strings are, respectively, $l_0 = pl$ and $l_1 = (1-p)l$, and the information rates (Shannon entropies per bit) are related as $h(S) = p\,h(S_0) = (1-p)\,h(S_1)$. To calculate the entropy rate of S_0 and S_1 we still use (5). Our simulations show that the correct decision on whether S_1 or S_0 is being used can decrease calculation times as well as increase convergence of (5) tremendously (data not shown here).

3. Results and discussion

3.1. Analytical results

We first discuss the case of t_m large enough so that the particle relaxes to equilibrium between measurements. In the limits of very large positive and large negative control values Δx, the external agent can predict the particle position (either on the left or the right side of Δx) with a high probability before performing the measurement. Consequently, the work related to Shannon entropy, W_info, approaches zero. On the other hand, W_info is maximal for $p = 0.5$, i.e., when the uncertainty of the measurement outcome is maximal, a situation that occurs for intermediate positive values of Δx, as can be seen in figure 2(a). $W_\mathrm{out} = pf_\mathrm{ext}L$ is linearly proportional to p,

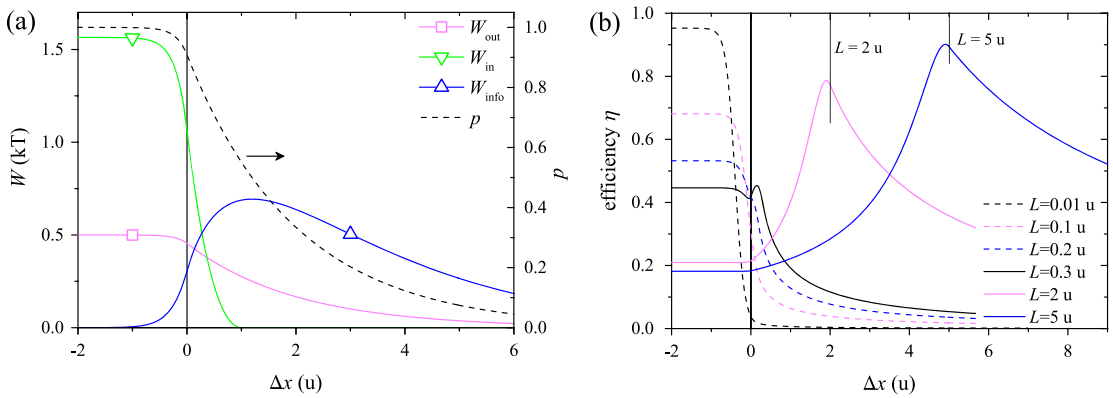

Figure 2. (a) System in equilibrium: probability distribution p, applied work W_{in}, gained potential energy W_{out} and the work related to Shannon entropy rate W_{info} as a function of the control value Δx with $f_b = 5$ kT/u, $f_{ext} = 0.5$ kT/u and $L = 1$ u. (b) High efficiency $\eta(\Delta x)$ can be reached both in the limit of very small L in the PS regime and in the limit of very large L in the intermixing regime of PS and BR. Efficiency peaks in the intermixing regime ($0 < \Delta x < L$). As a guide to the eye additional grid lines are shown at the positions $\Delta x = L$. The parameters $f_b = 10$ kT/u, $f_{ext} = 2$ kT/u are kept constant.

whereas W_{in} exhibits a more complicated dependence and vanishes for $\Delta x \geqslant L$. Notice that W_{info}, in contrast to W_{in} and W_{out}, does not depend on the step length L. As a consequence, efficiency as defined in (8) can have a maximum peak in the region $0 < \Delta x < L$ whereas it is constant for $\Delta x \ll 0$, see figure 2(b). We first investigate the asymptotic dependence of the efficiency for small and large Δx before we analyze the influence of L and f_b on the efficiency peak.

For $\Delta x \ll 0$ (PS regime), as described above, W_{info} approaches zero. Therefore, the efficiency in this regime can be estimated as

$$\eta(\Delta x \ll 0) \approx \frac{W_{out}}{W_{in}} \approx \frac{f_{ext} L}{\left(f_{ext} + f_b\right)L + f_b\left[-1 + \exp\left(-\beta f_{ext} L\right)\right]/\left(\beta f_{ext}\right)}, \tag{17}$$

which is independent of Δx.

For large Δx (BR regime), the probability of passing the control value approaches zero and for $\Delta x \gg L$, using the linear expansion, $-(1-p)\ln(1-p) \to p$ as $p \to 0$, we have

$$\eta(\Delta x \gg L) = \frac{W_{out}}{W_{info}} \approx \frac{\beta f_{ext} L}{\beta f_{ext}\Delta x + 1 - \ln\left[f_b/\left(f_b + f_{ext}\right)\right]} \approx \frac{L}{\Delta x}. \tag{18}$$

Equation (18) is valid for small p, thus not only in the case of large Δx, but also in case of large f_{ext} and small ratio $f_b/(f_b + f_{ext})$.

In the intermixing regime η has a peak for large step lengths, whereas it decreases as a function of Δx for small L. Unfortunately, the maximum $\eta(\Delta x^{max})$ can not be determined analytically. Nevertheless, $\eta(L = \Delta x)$ is a suitable approximation, assuming that the efficiency peak height depends only weakly on f_b, as can be seen in figure 4. With $W_{in}(\Delta x = L) = 0$ this leads to

$$\eta(\Delta x = L) = \frac{W_{out}}{W_{info}}. \tag{19}$$

Since p converges to a finite value $f_b/(f_b + f_{ext})$ when $\Delta x = L \to 0$, the efficiency approaches zero in this limit, as shown in figure 3. The peak itself will decrease and its position shift towards $\Delta x = 0$, as can be seen in figure 2(b). Next we analyze in more detail how the step length affects the efficiency.

High efficiencies can be reached in two limits. In figure 2(b), we observe that efficiencies close to 100% can be reached in the limit of both very small and very large step lengths L. For small step length, this is achieved through active pushing while for large L, high efficiency can only be achieved if information is utilized. In the case of very small L, the change of the system state s implies a small change in the potential, $V(x + L, s + 1) \cong V(x; s + 1)$, and η converges to a maximal 100% in the PS regime and approaches slowly zero for large control values Δx, as shown in figure 2(b). This is expected, since for very small L, the system is always very close to equilibrium and thus the process is almost reversible ($\eta \to 1$ for $L \to 0$). In the case of large

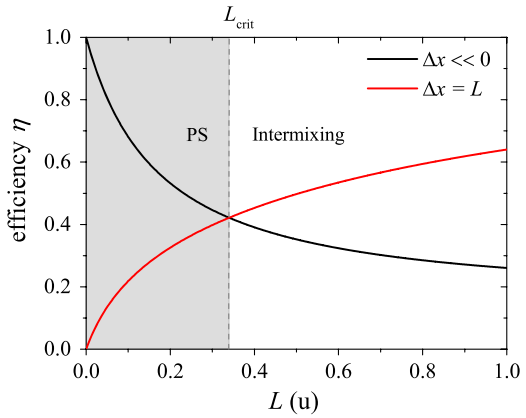

Figure 3. Efficiency of the PS ($\Delta x \to -\infty$, black) and the BR ($\Delta x = L$, red) regimes, as a function of L. Efficiency is larger in the pure PS regime for values $L < L_{crit}$ (shaded region). The parameter $f_b = 10$ kT/u is kept constant.

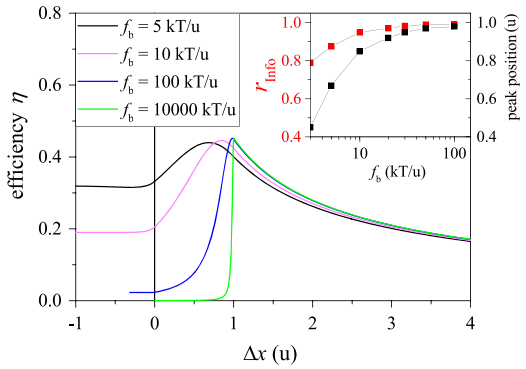

Figure 4. Only for very steep barriers, efficiency peaks in the pure BR regime; for lower f_b, efficiency is maximal in the intermixing regime. Efficiency is shown as a function of the control value Δx for various barrier forces. Increasing f_b shifts the efficiency peak towards the position of the next barrier $\Delta x = L$. The inset shows the peak position and the corresponding fraction r_{info} for various f_b. $f_{ext} = 0.5$ kT/u, $L = $ u.

L, a maximum efficiency close to 1 can be achieved at a control value $\Delta x^{max} \leqslant L$. The approximate expression for the peak position (19) approaches 0 for $L \to 0$ and 1 for $L \to \infty$.

In figure 3 we display the two expressions (17) and (19) and find that a critical length L_{crit} exists above which the intermixing of PS and BR becomes more efficient than pure PS. We define this length via the condition

$$\eta(\Delta x \ll 0) = \eta(\Delta x^{max}). \tag{20}$$

The comparison of efficiencies in figure 2(b) with figure 3 shows that the intersection of $\eta(\Delta x \ll 0)$ and $\eta(L)$ is, indeed, a good approximation of L_{crit}.

Dependency on f_b. A key result of this paper is that the peak position can be found in the intermixing regime of PS and BR. A closer look at the dependence of η on the barrier slope reveals the reason the maximum efficiency is found in this regime, figure 4. A decreasing barrier slope does not affect W_{out} and affects W_{info} only weakly. W_{in}, on the other hand, decreases significantly for $\Delta x < L$ and thus, efficiency increases, leading to a peak shift away from the pure BR ($\Delta x = L$) for decreasing f_b. The ratio to which information is used in the process compared to the complete work input $r_{info} = W_{info}/(W_{info} + W_{in})$ is thereby even less affected (see inset in figure 4). Interestingly, the maximum efficiency is only weakly affected by the decrease of f_b; instead, a peak broadening can be observed. This result implies that in systems in which the PS is relatively 'soft', efficiency is more robust against changes in Δx, for example, due to variation in the feedback mechanism. In other words, very high efficiencies might be reached even if information is not used in an optimal way.

3.2. Simulations

Numerical simulations of the Brownian dynamics are shown in figure 5. The efficiency exhibits the same features as in the case of large t_m, figure 5(a). Even though the correlation between the exact particle positions x_i and x_j are strong, we observed correlations between measurement results only for negative control values and

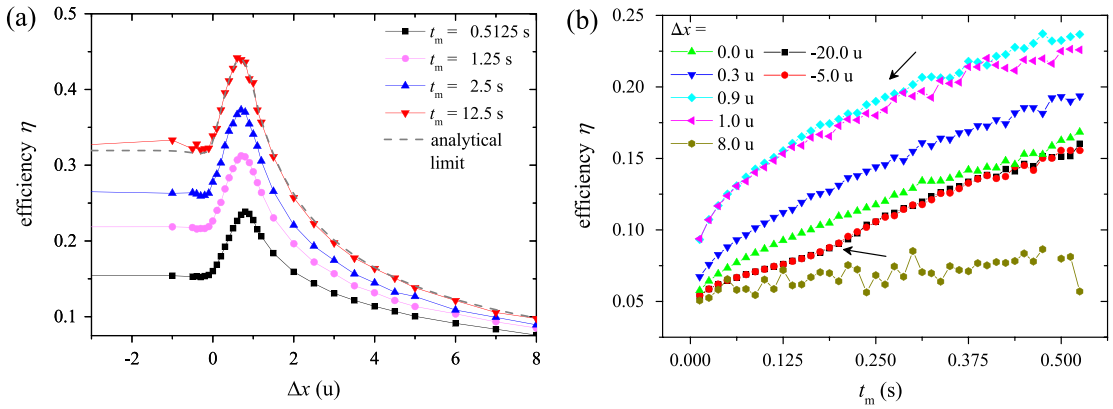

Figure 5. Brownian dynamics simulation: (a) efficiency as a function of the control value Δx (u) for different times t_m. For very long waiting times between the measurements, the system approaches equilibrium and efficiency reaches its analytical limit (dotted line). (b) For positive control values Δx, the general behavior is as in the analytical calculation, whereas lower frequencies lead to higher efficiencies and efficiency peaks for values $\Delta x < L$ (indicated by upper arrow). For negative control values, finite time effects can be found with a strong increase of efficiency above a certain t_m (compare black and red curves). The origin of the inflection in those curves (indicated by the lower arrow) is due to an increased switching probability. L is set to 1 u.

large t_m, figure 5(b) (see also appendix B). This is because most of the information is lost when it is stored as '0' and '1'. Consequently, a sudden increase in efficiency was observed only in the PS regime for a certain t_m, but not in the intermixing regime (inflection in figure 5(b)). For all positive Δx, the measurement results are uncorrelated (see figure B1(a) in appendix B). Therefore, W_{info} depends only on the probability distribution of the ensemble and can simply be extracted from (12).

4. The operating regime of biological motors

In section 3.1 we established that, in general, our model can operate in one of two regimes, separated by the critical step length L_{crit}. We now address the question in which length scale regime real biological motors as kinesin, myosin II, and myosin V operate: in the regime $L < L_{\text{crit}}$, where a PS is most efficient, or in the regime $L > L_{\text{crit}}$, where a mixture of BR and PS is most efficient?

4.1. Connection to molecular motors

To answer this question, the following simplifications and assumptions are made, in order to relate biological stepping motors to our simple one-dimensional model:

(i) A motors step size corresponds to L.

(ii) f_{ext} corresponds to the load acting on the motor; the maximal $f_{\text{ext}}^{\max}$ corresponds to the stall force, f_{stall}, measured in single molecule experiments.

(iii) In a real motor, f_{ext} and f_{b} are not independent, they are related through the available Gibbs free energy ΔG, see also appendix A. Assuming a pure PS mechanism without any other energy loss processes, the maximal possible W_{in} equals the available ΔG, leading to:

$$W_{\text{in}}^{\max} = \left(f_{\text{ext}}^{\max} + f_{\text{b}}^{\max}\right)L = \Delta G. \tag{21}$$

(iv) For effective rectification f_{b} should be larger than f_{ext}.

(v) Even though Δx scales in distance units in the model, it is important to keep in mind that it acts as the control parameter determining the ratio, r_{info}, to which information is used. Δx is not necessarily related to any distance in a real motor.

In molecular motors there is no external agent acting as a feedback control. Nevertheless, for effective processive motion of bipedal motors, it is crucial that the correct head unbinds at the correct time. The importance of this step-coordination was pointed out also by Bier [16], who mapped a flashing ratchet to the movement of kinesin. It is clear that this coordination needs some kind of internal feedback (information) about the system state,

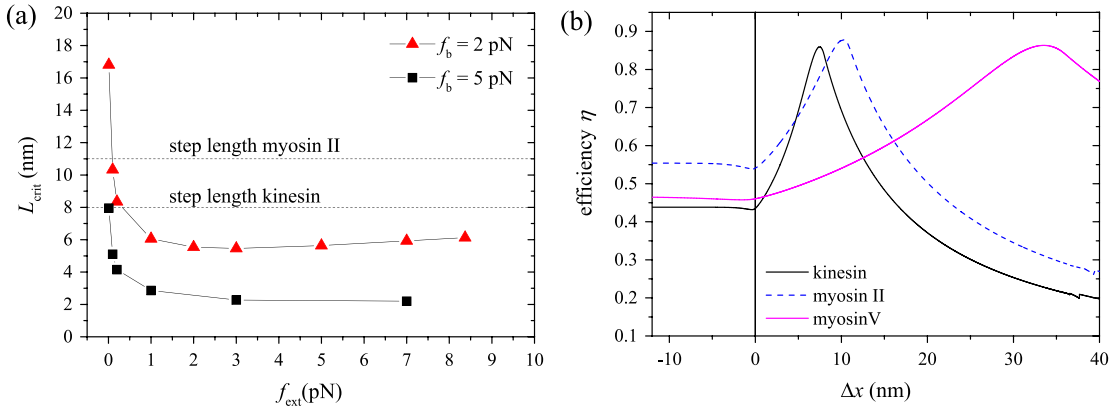

Figure 6. (a) L_{crit} as a function of the external force (load) f_{ext}. For all but the smallest load forces, f_{ext}, the step length of kinesin, myosin II, and myosin V is longer than L_{crit}. (For very small external forces, L_{crit} is strongly decreasing (efficiency is here very low), while it is slightly increasing for increasing f_{ext}.) f_b is kept constant at values 2 pN (red triangles) and 5 pN (black squares). (b) Calculated efficiency as a function of Δx for kinesin (dashed, blue), myosin II (magenta), and myosin V (black). All three motors show higher efficiency in the intermixing regime than for pure PS. The values used for f_b, L, f_{ext} are given in table 1.

Table 1. Values for L, f_{ext} and f_b that are used in figure 6(b). f_{ext} corresponds to reported stall forces f_{stall} and f_b was determined using (21) and $\Delta G^{ATP} \approx 50$ kJ mole^{-1}. r_{info} is calculated at the efficiency maximum $\eta(\Delta x^{max})$; rectification is the dominant process with about 97% for all three motor types.

Motor	L (nm)	f_{ext} (pN)	f_b (pN)	Δx^{max} (nm)	r_{info} (%)	$\eta(\Delta x^{max})$ (%)	η^* (%)
Kinesin	8 [19]	4.2 [19]	6.18	7.5	97	86	40.5
Myosin II	11	4	3.55	10.2	96	88	53.0
Myosin V	36	1	1.3	33.8	98	86	43.4

with an associated information cost. An in-detail mapping of a possible feedback mechanism of the complex real biological motors exceeds the scope of this article, but we refer to an analysis of biochemical copying of information that can be found in [17]. The efficiency of information processing is addressed by Barato *et al* in [18]. In bipedal motors, the feedback mechanism might be thought of as a change of the potential landscape, leading to different binding and unbinding rates of front and rear head. The mechanisms of how exactly these asymmetries are introduced are under discussion; one possible factor could be mechanical strain, as suggested for myosin V [7, 8]. Here we focus on the establishing the length scale regime, in which typical molecular motors operate.

4.2. Critical step length for kinesin, myosin II, and myosin V

We start our analysis by comparing L_{crit}, determined at constant barrier forces of 2 and 5 pN for varying loads between 0.02 and 8 pN in figure 6(a). The barrier forces are chosen so that their values have magnitudes relevant for molecular motors, assuming that $f_b > f_{ext}$, where f_{ext} is bounded by f_{stall}. Stall forces of 2 and 5 pN are in the range reported for kinesin and myosin II [19–21]. The load f_{ext} is varied independently. For all but the very small loads, $f_{ext} < 0.3$ pN, L_{crit} is far below the step length of the kinesin, myosin II and myosin V motors, (8, 11, and 36 nm, respectively), suggesting that all three motors gain efficiency through the intermixing of PS and BR during their operation.

To compare more accurately a few assumptions about f_{ext} and f_b have to be made as stated in section 4.1. Kinesin is one of the most intensively studied protein motors with f_{stall} between 4.2 and 5 pN [19, 20, 22–24]. For an example calculation we use $f_{ext}^{max} = 4.2$ pN. With $\Delta G^{ATP} \approx 50$ kJ mole$^{-1} \approx 83$ pN nm (at body temperature 37 °C), (21) leads to $f_b^{max} = 6.18$ pN. The resulting efficiency plot is shown in figure 6(b), together with examples for myosin II and myosin V (all parameters used are listed in table 1). The maximal possible efficiencies $\eta(\Delta x^{max})$ for all three protein motors are between 86 and 88%. If the investigated motors perform at $\eta(\Delta x^{max})$, our analysis suggests that they operate in the intermixing regime, where both rectification of fluctuations and PS is utilized, see table 1.

Notice that various types of efficiencies have been defined in the literature and estimated for molecular motors. For example efficiencies obtained through velocity-force measurements ($\eta^* = -f_{ext} L/\Delta G^{ATP}$) help us to estimate the strength of the coupling between the chemical Gibbs free energy ΔG^{ATP} and the motor motion. Viscosity–velocity measurements and the resulting efficiency can determine whether the motor operates with a constant force. In our case, efficiency measures how well the energy that is consumed in the conformational

chance can be used to create forward motion and generate a force. As defined in (8), η with its dependency on Δx, considers whether the rectification of Brownian fluctuations or a PS will do this more efficiently. To provide context we have also calculated $\eta^{\star}$. These values are between 40.5 and 53.0%, table 1.

The above analysis of biological motors neglects possible correlations and their effect on W_{info}. This is justified by our numerical simulations showing that in such a system (which distinguish only between 'bound to the next binding side' or 'not bound') correlations do not occur (compare appendix B) and thus information cost is determined by the equilibrium distribution $\rho(x, s)$. Our analytical results are valid for times large enough to let the system reach equilibrium, which can be expected since equilibrium will be reached in picoseconds whereas the time scale of the chemical transitions of the motor cycle is in the regime of milliseconds [25].

It should also be noted that this article focuses on the energy efficiency; however, numerical simulations can be used to estimate the velocity of motors operating in different ranges between pure PS, intermixture of PS and BR or pure BR. We simulated the average time of a cycle for a motor with step length 8 nm and the energetically possible combinations of f_{ext} and f_{b} (as described above) if the motor is operating at its maximum efficiency ($\Delta x = 7.5$ nm). The resulting velocities lay within tens to hundreds of nm per second and are thus well within the range that can be found in literature for kinesin [20, 24, 26].

5. Conclusion

Molecular motors are described as BR or as motors operating according to a PS mechanism. While it is difficult to clearly distinguish whether a given molecular motor steps by BR or PS (or both), we show that for typical step lengths of processive, bipedal, biological motors, the mixing of BR and PS provides the highest efficiency. Although, for a molecular motor in a biological context, other performance parameters, such as processivity, load-force tolerance and maximum power, can be equally or more important than efficiency, it is nevertheless noteworthy that our results suggests that kinesin as well as examples from the myosin family are operating in a regime, where fluctuations can be used very efficiently (for kinesin $r_{\mathrm{info}} \approx 97\%$). Furthermore, the model proposed in this investigation can be used to simulate a bead moving in an optical line trap under feedback control, a possible realization of a Maxwell's demon [27]. A similar system has been studied by Toyabe *et al* [28], but our system has the advantage that it allows us to investigate not only the 'pure Maxwell's demon', but also the impact of feedback delay and PS.

Acknowledgments

The research leading to these results has received funding from the European Union Seventh Framework program (FP7/2007–2013) under grant agreement nr 308850 (project acronym INFERNOS) and by the Swedish Research Council. J M R P gratefully acknowledges the Pufendorf Institute at Lund university for its hospitality at the beginning of this project and financial support from the Spanish MINECO Grant ENFASIS (FIS2011-22644).

Appendix A. Illustration of a PS

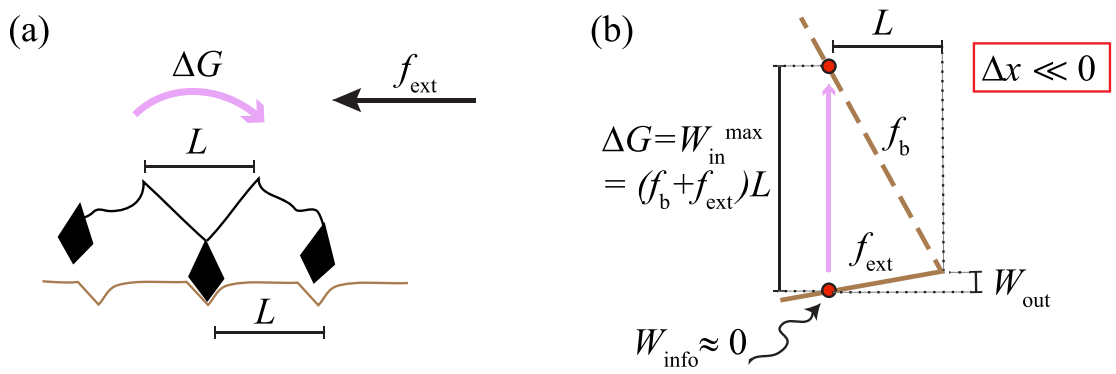

Figure A1. Power-stroke. (a) Schematics of a bipedal molecular motor (black) walking along a track (brown) using power-stroke; inspired by figure 3 in [16]. The available Gibbs free energy ΔG is used for a conformational change that brings the former rear head close to the next binding side in the front, overcoming the distance L, which corresponds to the step length. (b) Power-stroke regime in the described model ($\Delta x \ll 0$). ΔG is equal to the energy consumed due to active pushing, $W_{\mathrm{in}}^{\mathrm{max}}$, that can be done against the external force $f_{\mathrm{ext}} \approx f_{\mathrm{stall}}$. $W_{\mathrm{info}} = 0$.

Appendix B. Correlations

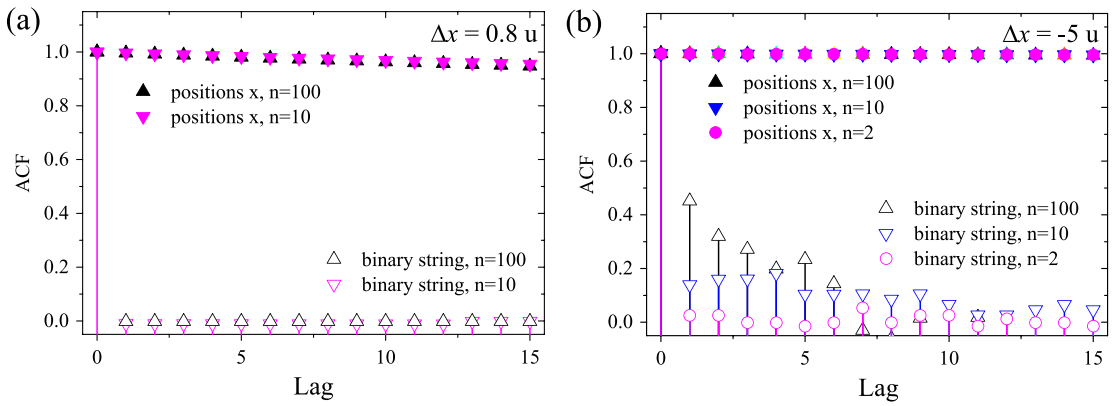

Figure B1. Autocorrelation function (ACF) of the particle position x (filled symbols) and the measurement outcomes, stored as '0' if the particle has not passed and '1', if the particle has passed the control value Δx at the time of measurement in a binary string (unfilled symbols), for positive (a) and negative (b) Δx, respectively. The correlation of the positions are in all cases very high. As can be expected, for positive Δx (a), the binary string shows no correlations, because the measurement outcomes rely solely on the Brownian motion. For negative Δx (b), on the other hand, an increase in correlations within the string can be found for increasing numbers of time steps, n, between measurements ($\rightarrow$ increasing t_m). This is because the particle is driven towards the next checkpoint at position Δx by f_b, whereas the fluctuating part of the motion averages out for long waiting times between measurements (large n). L is set to 1 u, $f_{ext} = 0.5$ kT/u, $f_b = 5$ kT/u and $t_m = n0.0125$ s.

References

[1] Howard J 2006 *Curr. Biol.* **16** R517–9
[2] Huxley A F 1957 *Prog. Biophys. Biophys. Chem.* **7** 255–318
[3] Wang H and Oster G 2002 *App. Phys.* A **75** 315–23
[4] Galburt E A, Parrondo J M and Grill S W 2011 *Biophys. Chem.* **157** 43–47
[5] Cao F and Feito M 2009 *Phys. Rev.* E **79** 041118–1
[6] Parrondo J M R, Horowitz J M and Sagawa T 2015 *Nat. Phys.* **11** 131–9
[7] Rief M, Rock R S, Mehta A D, Mooseker M S, Cheney R E and Spudich J A 2000 *Proc. Natl Acad. Sci. USA* **97** 9482–6
[8] Purcell T J, Sweeney H L and Spudich J A 2005 *Proc. Natl Acad. Sci. USA* **102** 13873–8
[9] Gennerich A and Vale R D 2009 *Curr. Opin. Cell Biol.* **21** 59–67
[10] Astumian R D 2010 *Biophys. J.* **98** 2401–9
[11] Parrondo J M R and de Cisneros B J 2002 *Appl. Phys.* A **75** 179–91
[12] Horowitz J M, Sagawa T and Parrondo J 2013 *Phys. Rev. Lett.* **111** 010602
[13] Bauer M, Abreu D and Seifert U 2012 *J. Phys. A: Math. Theor.* **45** 162001
[14] Cover T M and Thomas J A 2006 *Elements of Information Theory* 2nd edn (Hoboken, NJ: Wiley) pp 13–55
[15] Roldán E and Parrondo J M R 2010 *Phys. Rev. Lett.* **105** 150607
[16] Bier M 2007 *BioSystems* **88** 301–7
[17] Ouldridge T E, Govern C C and ten Wolde P R 2015 (arXiv: 1503.00909v2)
[18] Barato A C, Hartich D and Seifert U 2015 *New J. Phys.* **16** 103024
[19] Hunt A J, Gittes F and Howard J 1994 *Biophys. J.* **67** 766–81
[20] Svoboda K and Block S M 1994 *Cell* **77** 773–84
[21] Finer J T, Simmons R M and Spudich J A 1994 *Nature* **368** 113–9
[22] Meyhöfer E and Howard J 1995 *Proc. Natl Acad. Sci. USA* **92** 574–8
[23] Svoboda K, Schmidt C F, Schnapp B J and Block S M 1993 *Nature* **365** 721–7
[24] Coppin C M, Pierce D W, Hsu L and Vale R D 1997 *Proc. Natl Acad. Sci. USA* **94** 8539–44
[25] Leibler S and Huse D A 1993 *J. Cell Biol.* **121** 1357–68
[26] Schnitzer M J, Visscher K and Block S M 2000 *Nat. Cell Biol.* **2** 718–23
[27] Maxwell J C 1871 *Theory of Heat* (London: Longmans Green)
[28] Toyabe S, Sagawa T, Ueda M, Muneyuki E and Sano M 2010 *Nat. Phys.* **6** 988–92